Order−Disorder Transition, Microdomain Structure, and Phase Behavior in Binary Mixtures of Low Molecular Weight Polystyrene-*block*-polyisoprene Copolymers

Daisuke Yamaguchi and Takeji Hashimoto*

Department of Polymer Chemistry, Gradate School of Engineering, Kyoto University, Kyoto 606-01, Japan

Chang Dae Han,* Deog Man Baek,† and Jin Kon Kim‡

Department of Polymer Engineering, The University of Akron, Akron, Ohio 44325

An-Chang Shi

Xerox Research Center at Canada, 2660 Speakman Drive, Missisauga, Ontario, Canada L5K 2L1

Received January 17, 1997; Revised Manuscript Received July 22, 1997[⊗]

ABSTRACT: Order−disorder transition, microdomain structure, and phase behavior in binary mixtures of low molecular weight polystyrene-*block*-polyisoprene (SI diblock) copolymers were investigated. For the study, four SI diblock copolymers were synthesized, namely (i) SI-Q having a weight-average molecular weight (M_w) of 2.8×10^4 and polystyrene volume fraction (f) of 0.186, (ii) SI-R having $M_w = 1.5 \times 10^4$ and $f = 0.508$, (iii) SI-S having $M_w = 1.76 \times 10^4$ and $f = 0.372$, and (iv) SI-M having $M_w = 1.55 \times 10^4$ and $f = 0.626$. Then binary mixtures of SI-Q and SI-R and binary mixtures of SI-M and SI-S, with various compositions, were prepared via solvent casting. The order−disorder transition of the binary mixtures was investigated using rheology and small-angle X-ray scattering (SAXS), respectively. Also investigated was the microdomain structure of the binary mixtures using SAXS and transmission electron microscopy (TEM). Experimentally determined phase diagrams are compared with predictions based on a self-consistent mean-field theory.

1. Introduction

In the past, some experimental studies have been reported on the order−disorder transition (ODT) in mixtures of block copolymers and homopolymers,[1−5] but very little on binary mixtures of block copolymers. Also, many studies have been reported on the microdomain structure,[6−17] phase behavior,[18−25] and spatial distribution of each component[26−28] in binary mixtures of block copolymers and homopolymers, but fewer studies on the microdomain structure,[29−33] phase equilibria,[34−37] and component distribution[29,36−38] in binary mixtures of diblock copolymers.

In their experimental study, using transmission electron microscopy (TEM), Hashimoto et al.[29,33] observed that when mixing equal amounts of two polystyrene-*block*-polyisoprene (SI diblock) copolymers, one having hexagonally-packed polystyrene (PS) cylinders in the matrix of polyisoprene (PI) and the other having hexagonally-packed PI cylinders in the matrix of PS, the mixture had a single microdomain morphology of alternating lamellae of PS and PI. They speculated, however, on the possibility of having macrophase separation as well when mixing two block copolymers having different compositions and/or different molecular weights. In subsequent studies,[31−33] they indeed observed both microphase and macrophase separations in binary mixtures of SI diblock copolymers. Using TEM and scanning electron microscopy, Ishizu et al.[30] also observed both microphase and macrophase separations, depending upon the volume fraction of binary block sequences and the casting conditions employed, in binary mixtures of an SI diblock copolymer and a polystyrene-*block*-poly(2-vinylpyridine) copolymer. Using neutron reflectivity Mayes et al.[38] observed nonuniform distributions of components in microphase-separated binary mixtures of polystyrene-*block*-poly(methyl methacrylate) (PS-*block*-PMMA) copolymers; namely, the shorter copolymer chains were localized to the PS/PMMA interface regions while the longer copolymer chains stayed at the domain centers. It is clear from the recent theoretical studies of Shi and Noolandi[36,37] that the microdomain structures and phase behavior in binary mixtures of AB-type diblock copolymers are indeed very complex.

In this study we synthesized a series of low molecular weight SI diblock copolymers and then prepared binary mixtures. Using the mixtures we investigated their ODT, microdomain structure, and phase behavior, using rheology, small-angle X-ray scattering (SAXS), and TEM. Low molecular weight block copolymers were needed in order to be able to determine the order−disorder transition temperature (T_{ODT}) of such mixtures at sufficiently low temperatures, such that the block copolymers would be thermally stable during the experiment. In this paper we will first present the results of T_{ODT}, which were obtained from both rheology and SAXS, for the binary mixtures prepared in this study and then discuss the microdomain structures, which were determined by TEM and SAXS, for the binary mixtures. Finally we will compare experimental results of phase diagrams and microdomain structure with predictions made by a self-consistent mean-field theory.

† Present address: Polymer Laboratory, Research Center, Daelim Industry Ltd., Science Town, Taijeon 305-343, Korea.

‡ Present address: Department of Chemical Engineering, Pohang University of Science and Technology, Pohang, Kyungbuk 790-784, Korea.

⊗ Abstract published in *Advance ACS Abstracts,* September 1, 1997.

S0024-9297(97)00050-8 CCC: $14.00

Table 1. Molecular Characteristics of the SI Diblock Copolymers Investigated in this Study

sample code	$M_w \times 10^{-4}$	M_w/M_n	wt % PS	N_{PS}[a]	N_{PI}[b]	f_{PS}[c]	r[d]
SI-M	1.55	1.06	66.7	93.64	71.5	0.626	169.4
SI-S	1.76	1.06	40.9	67.25	148.6	0.372	207.1
SI-Q	2.80	1.06	21.2	53.82	305.9	0.186	330.0
SI-R	1.50	1.07	54.5	73.37	93.7	0.508	170.4

[a] N_{PS} is the weight-average degree of polymerization of PS blocks. [b] N_{PI} is the weight-average degree of polymerization of PI blocks. [c] f_{PS} is the volume fraction of PS block in the SI diblock copolymer at 25 °C. [d] $r = (v_{PS}/v_o)N_{PS} + (v_{PI}/v_o)N_{PI}$ which is the effective degree of polymerization in which $v_o = (v_{PS}v_{PI})^{1/2}$ with v_{PS} and v_{PS} being the molecular volumes of PS and PI blocks, respectively.

2. Experimental Section

2.1. Materials. Four SI diblock copolymers, designated as SI-Q, SI-R, SI-S, and SI-M, were synthesized via anionic polymerization in our laboratory. Table 1 gives a summary of the molecular characteristics of the block copolymers synthesized. In the polymerization, cyclohexane was used as the solvent and *sec*-butyllithium as the initiator to first polymerize isoprene monomer anionically and then to copolymerize styrene monomer with this living polyisoprene to form an SI diblock copolymer. The number-average molecular weight (M_n) of the SI diblock copolymers synthesized was determined using membrane osmometry, the polydispersity index (M_w/M_n) using gel permeation chromatography, and the weight fraction of polystyrene block using ultraviolet spectroscopy at a wavelength of 254 nm. Nuclear magnetic resonance spectroscopic analysis indicated that the polyisoprene consisted of about 6 wt % 3,4-polyisoprene, about 94 wt % 1,4-polyisoprene, and no detectable amount of 1,2-polyisoprene in the SI diblock copolymers synthesized.

We prepared two binary systems, SI-Q/SI-R mixtures and SI-M/SI-S mixtures, each having various compositions. The rationale for having chosen these two binary systems is as follows. Since, on the basis of block copolymer composition, SI-Q is expected to have hexagonally-packed cylinders of PS in the matrix of PI, and SI-R is expected to have alternating layers of PS and PI, we would expect that combinations of these two block copolymers might give rise to a microdomain structure between cylinders and lamellae if the linear additivity rule for weight fractions is applicable to predict the resulting microdomain structure. On the other hand, since, on the basis of block copolymer composition, SI-S is expected to have hexagonally-packed cylinders of PS in the matrix of PI and SI-M is expected to have hexagonally-packed cylinders of PI in the matrix of PS, we would expect that combinations of these two block copolymers might give rise to alternating layers of PS and PI if the linear additivity rule for weight fractions is applicable to predict the resulting microdomain structure.

2.2. Sample Preparation. Samples were prepared by first dissolving a predetermined amount of neat block copolymer or a binary mixture of block copolymers in toluene in the presence of an antioxidant (Irganox 1010, Ciba-Geigy Group) and then slowly evaporating the solvent. The evaporation of toluene was carried out initially in a fume hood at room temperature for a week and then in a vacuum oven at 40 °C for 3 days. The last trace of toluene was removed by drying the samples in a vacuum oven at elevated temperature by gradually raising the oven temperature up to 10 °C above the glass transition temperature (T_g) of the PS phase in each block copolymer. The drying of the samples was continued, until there was no further change in weight. Finally, the samples were annealed for 10 h at the same temperature as described above. In general, annealing increases the degree of ordering in microdomain structures.

2.3. Rheological Measurement. A Model R16 Weissenberg rheogoniometer (Sangamo Control Inc.) in the cone−plate (25 mm diameter plates and 4° cone angle with a 160 μm gap between the cone tip and the plate) configuration was used to measure the dynamic storage modulus (G') and dynamic loss modulus (G'') as functions of angular frequency (ω) at various temperatures, for each of the block copolymers or binary mixtures thereof. Temperature control was satisfactory to within ±1 °C. In the oscillatory shear flow measurements a fixed strain of 0.003, which was well within the linear viscoelastic range of the materials investigated, was used. All experiments were conducted in the presence of nitrogen in order to preclude oxidative degradation of the samples.

2.4. Small-Angle X-ray Scattering (SAXS). SAXS experiments were conducted, under a nitrogen atmosphere in the heating cycle, using an apparatus described in detail elsewhere,[39] which consists of a 18-kW rotating-anode X-ray generator operated at 45 kV × 400 mA (MAC Science, Yokohama City, Japan), a graphite crystal for incident-beam monochromatization, a 1.5-m camera, and a one-dimensional position-sensitive proportional counter. The specimens were annealed as described in Section 2.2, and they were subjected to a rapid cooling to room temperature. The Cu Kα line (=0.154 nm) was used. The SAXS profiles were measured in-situ as a function of temperature and were corrected for absorption, air scattering, and background scattering arising from thermal diffuse scattering, as well as slit-height and slit-width smearing.[40] The absolute SAXS intensity was obtained using the nickel-foil method.[41] In the present study, temperature dependence of SAXS profiles was obtained with a large temperature increment of 10 °C (referred to hereafter as the low temperature-resolution SAXS experiment) and also with a small temperature increment of either 1 or 2 °C (referred to hereafter as the high-temperature-resolution SAXS experiment) in a temperature enclosure which was sealed by nitrogen gas. This new temperature enclosure and temperature controller enabled us to control the sample temperature to within ±0.002 °C. The specimen was held for 1 h after reaching a preset temperature and then subjected to SAXS measurement for 1 h at that temperature, unless stated otherwise. Then the specimen temperature was increased by a specified increment, and the above process was repeated. We found small hysteresis effects in the mixtures investigated; namely, the data obtained in the heating cycle were *approximately* the same as those obtained in the cooling cycle for the time scale of observation employed in our experiments. The T_{ODT}s determined during heating and cooling agree within 3 °C.

2.5. Transmission Electron Microscopy (TEM). The microdomain structures formed in the binary mixtures, the SI-Q/SI-R and SI-M/SI-S mixtures, were investigated using TEM. For this, ultrathin sectioning was performed by cryoultramicrotomy at −100 °C, below the glass transition temperature (T_g = −68 °C) of PI, to attain the rigidity of the specimen, using a Reichert Ultracut E low-temperature sectioning system. A Hitachi H-600 transmission electron microscope operated at 100 kV was used to obtain micrographs of the specimens stained with osmium tetraoxide.

3. Results and Discussion

3.1. Order−Disorder Transition Investigated by Rheology. In a previous paper[42] we already reported that the T_{ODT} of SI-Q is 95 °C and the T_{ODT} of SI-R is 100 °C. Figure 1 gives log G' vs log ω and log G'' vs log ω plots, and Figure 2 gives log G' vs log G'' plots for 90/10 SI-Q/SI-R mixture at various temperatures. It is of interest to observe in Figure 1 that at 100 °C the slope of log G' vs log ω and log G'' vs log ω plots in the terminal region is very low (less than 0.5) and a sudden downward displacement in log G' vs log ω plots occurs at 110 °C. Using the rheological criterion advocated by Han and co-workers,[43−45] we determine the T_{ODT} of 90/10 SI-Q/SI-R mixture to be 115 °C from Figure 2, and the T_{ODT} of 80/20 SI-Q/SI-R mixture to be 120 °C from Figure 3. Similar results obtained for other blend ratios are not shown here. Table 2 gives a summary of the values of T_{ODT} of SI-Q/SI-R mixtures investigated in this study.

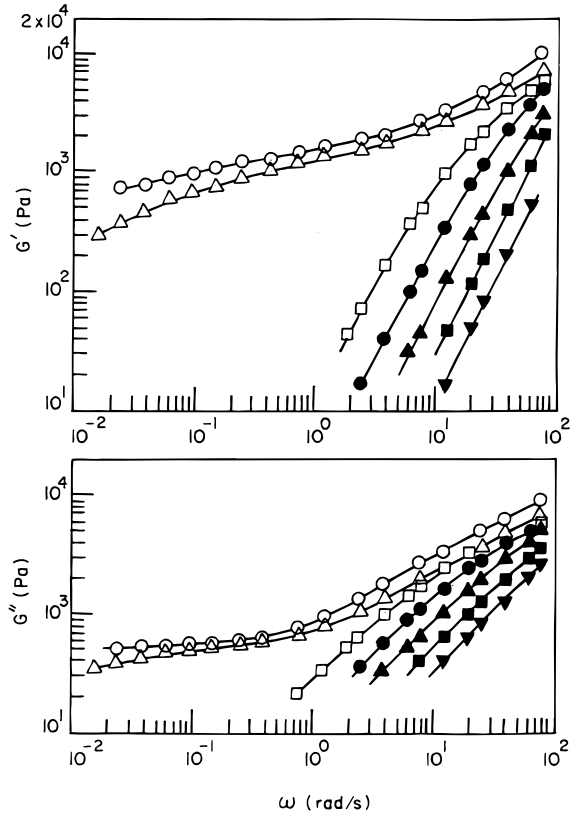

Figure 1. Plots of log G' vs log ω and log G'' vs log ω for the 90/10 SI-Q/SI-R mixture at various temperatures: (○) 100 °C; (△) 105 °C; (□) 110 °C; (●) 115 °C; (▲) 120 °C; (■) 125 °C; (▼) 130 °C.

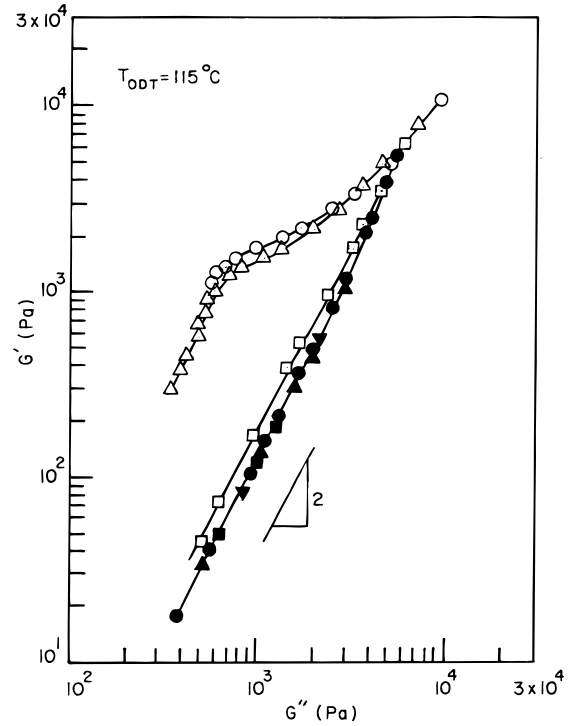

Figure 2. Plots of log G' vs log G'' for the 90/10 SI-Q/SI-R mixture at various temperatures: (○) 100 °C; (△) 105 °C; (□) 110 °C; (●) 115 °C; (▲) 120 °C; (■) 125 °C; (▼) 130 °C. The T_{ODT} of this mixture is determined to be ca. 115 °C.

In a previous paper[42] we already reported that the T_{ODT} of SI-S is 80 °C. On the other hand, we observe from Figure 4 that SI-M is in the disordered state at 85 °C, the lowest experimental temperature employed, because the torque was too high for us to be able to take

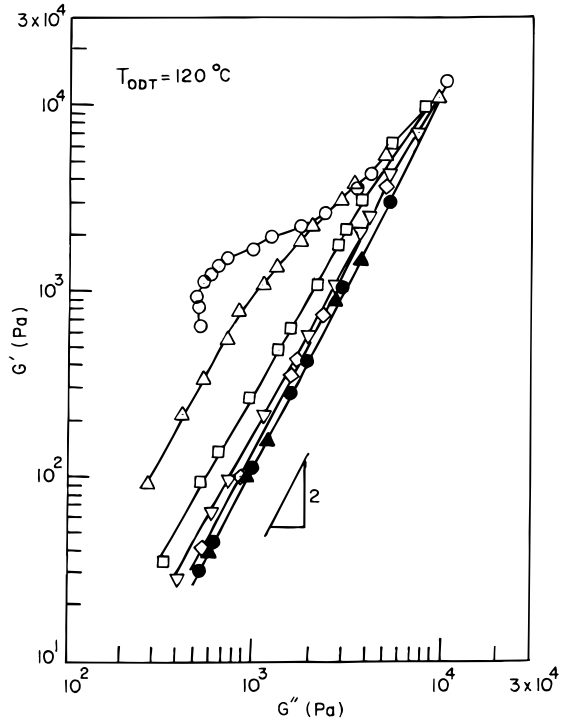

Figure 3. Plots of log G' vs log G'' for the 80/20 SI-Q/SI-R mixture at various temperatures: (○) 95 °C; (△) 100 °C; (□) 105 °C; (▽) 110 °C; (◇) 115 °C; (●) 120 °C; (▲) 125 °C. The T_{ODT} of this mixture is determined to be ca. 120 °C.

Table 2. Summary of T_{ODT}s Determined from Rheological and SAXS Measurements for SI-Q/SI-R and SI-M/SI-S Mixtures

	T_{ODT} (°C)	
sample code	rheology	SAXS
(a) SI-Q/SI-R Mixtures		
SI-Q	95	82−91
SI-R	100	89−90
90/10 SI-Q/SI-R	115	98−100
80/20 SI-Q/SI-R	120	90−100
60/40 SI-Q/SI-R	115	
50/50 SI-Q/SI-R	110	
40/60 SI-Q/SI-R	110	90−92
20/80 SI-Q/SI-R	105	
(b) SI-M/SI-S Mixtures		
SI-S	80	61−69
SI-M	a	below T_g
80/20 SI-M/SI-S	a	below T_g
75/25 SI-M/SI-S		80−90
70/30 SI-M/SI-S	105	86−89
65/35 SI-M/SI-S		91−99
60/40 SI-M/SI-S	115	
50/50 SI-M/SI-S	118	96−98
40/60 SI-M/SI-S	118	
20/80 SI-M/SI-S	105	87−88
10/90 SI-M/SI-S	95	

[a] The sample was found to be in the disordered state at temperatures as low as 85 °C the lowest experimental temperature, below which rheological measurements were not possible because the torque was too high to be measurable. This seems to indicate that the T_{ODT} might be below the T_g of the PS phase in the specimen.

rheological measurements at temperatures below 85 °C. This was due to the fact that the glass transition temperature (T_g) of the PS phase in SI-M was 70 °C as determined by differential scanning calorimetry. Figure 5 gives log G' vs log G'' plots for 80/20 SI-M/SI-S mixture at various temperatures, showing that this mixture is still in the disordered state over the range of temperatures investigated. However, when the amount of SI-S

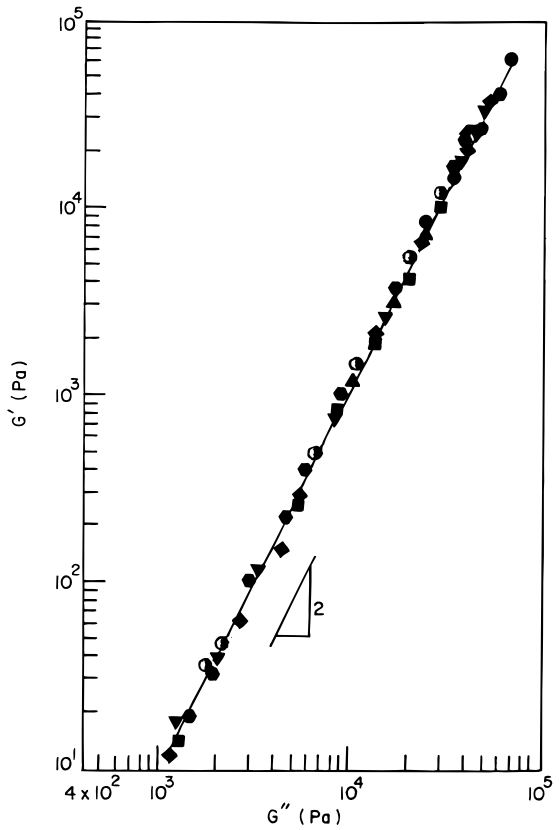

Figure 4. Plots of log G' vs log G'' for SI-M at various temperatures: (●) 85 °C; (▲) 90 °C; (■) 95 °C; (▼) 100 °C; (◆) 105 °C; (⬢)110 °C; (◑) 115 °C. This block copolymer is determined to be homogeneous over the entire range of temperatures investigated.

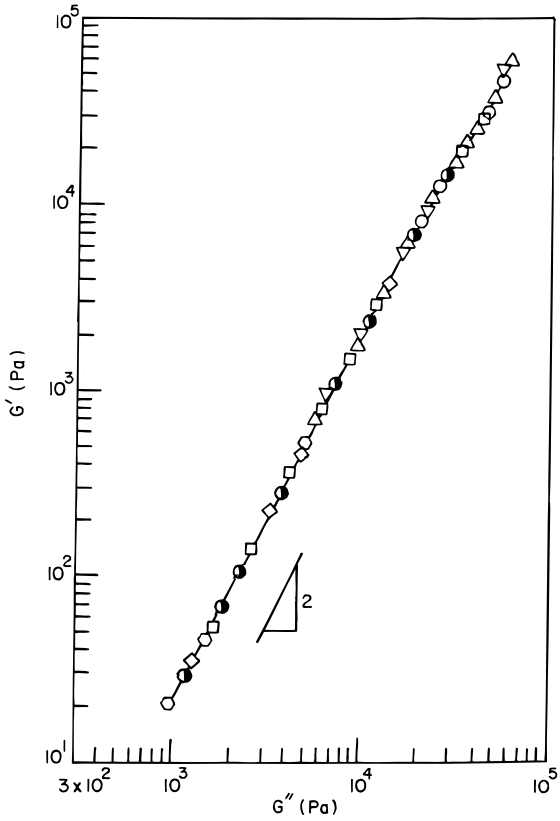

Figure 5. Plots of log G' vs log G'' for the 80/20 SI-M/SI-S mixture at various temperatures: (○) 85 °C; (△) 90 °C; (□) 95 °C; (▽) 100 °C; (◇) 105 °C; (⬡) 110 °C; (◑) 115 °C. This mixture is determined to be homogeneous over the entire range of temperatures investigated.

is increased further to yield 70/30 SI-M/SI-S mixture, as can be seen in Figure 6, we observe that this mixture has microdomains and has the T_{ODT} of ca. 105 °C. This indicates that the addition of SI-S to SI-M induced microphase separation in the 70/30 SI-M/SI-S mixture. Using log G' vs log G'' plots, we determined the T_{ODT}s of 60/40, 50/50, 40/60, 20/80, and 10/90 SI-M/SI-S mixtures, the results of which are summarized in Table 2.

3.2. Order−Disorder Transition Investigated by SAXS. Figure 7 gives SAXS profiles near the first-order scattering maximum, obtained by high temperature-resolution experiment, for the 20/80 SI-M/SI-S mixture at temperatures of 80, 82, 83, 84, 85, 86, 87, 88, 89, and 90 °C (near ODT). The temperature dependence of the profiles clearly reveals that the peak breadth sharply broadens and the peak intensity decreases upon increasing temperature between 84 and 88 °C. In order to facilitate an analysis of the SAXS profiles, in Figure 8 are given plots of the reciprocal of the peak intensity ($1/I_m$) vs the reciprocal of the absolute temperature ($1/T$) on the semi-logarithmic scale for SI-M/SI-S mixtures. It should be mentioned that in this paper we define I_m by the maximum intensity of the SAXS profile and not by the intensity of the SAXS profile at a certain value of q. Therefore an increase (or a decrease) of the values of I_m with $1/T$ in an ordered state, as will be seen below, is not related to the peak shift. If I_m were defined by the intensity of the SAXS profile at a certain fixed value of the wavevector q, the peak shift would possibly cause an increase (or a decrease) of $1/I_m$ with $1/T$.

For precise determination of T_{ODT}, we first employed low-temperature-resolution SAXS experiment for a rough estimation of T_{ODT}. We then applied high-temperature-resolution SAXS experiment to pinpoint T_{ODT} over a narrower temperature range around the predetermined T_{ODT}. Even the data shown in Figure 8, obtained with a low-temperature-resolution SAXS experiment, shows a sharp discontinuity in the log ($1/I_m$) vs $1/T$ plot at around T_{ODT} for each mixture, except for the data shown in part c: T_{ODT} = 60−70, 80−90, 95−100, 90−100, and 80−90 °C for 0/100, 20/80, 50/50, 65/35, and 70/30 SI-M/SI-S mixtures, respectively. A close observation of the data for the 75/25 SI-M/SI-S mixture appears to indicate its T_{ODT} = 80−90 °C. It should be noted that the data at 85 and 90 °C for the 70/30 SI-M/SI-S mixture (◆) and those at 80 and 90 °C (○) for the 75/25 SI-M/SI-S mixture were taken after a prolonged preheating time of 6 h (instead of 1 h) at the specified temperature. Otherwise the discontinuous increase of $1/I_m$ with decreasing $1/T$ was found to be much smaller than that shown in Figure 8. We expect that T_{ODT}s for the 80/20 SI-M/SI-S mixture and neat SI-M are lower than their T_gs.

It is reassuring to observe here that the SAXS results for both neat block copolymer SI-M and 80/20 SI-M/SI-S mixture are consistent with the rheological results given in Figures 4 and 5, indicating that they are in the disordered state over the entire range of temperatures investigated.

A small drop of $1/I_m$ between 80 and 90 °C observed for the 75/25 SI-M/SI-S mixture may be due to the fact that T_{ODT} (≅80−90 °C) for this system is very close to its T_g. This makes its ordering process very slow and hence the small drop of $1/I_m$ at T < T_{ODT} over the time scale of our observations.

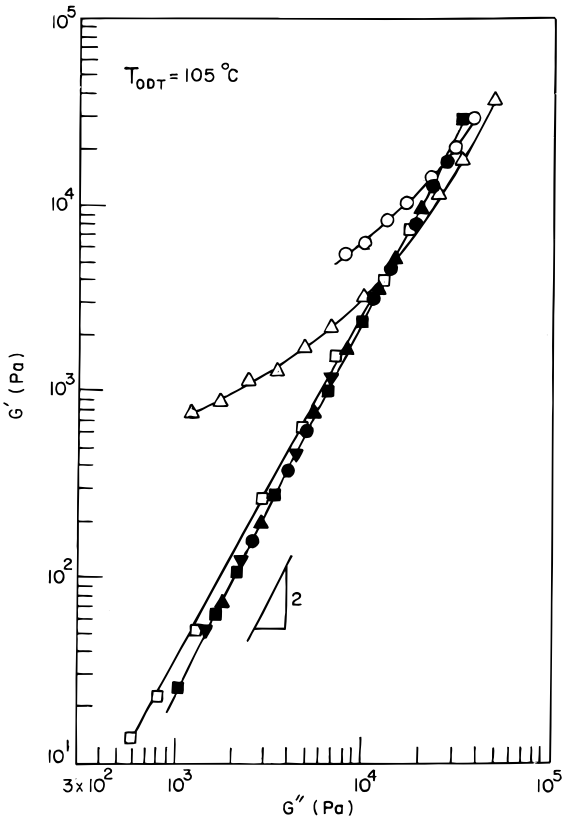

Figure 6. Plots of log G' vs log G'' for the 70/30 SI-M/SI-S mixture at various temperatures: (○) 90 °C; (△) 95 °C; (□) 100 °C; (●) 105 °C; (▲) 110 °C; (■) 115 °C; (▼) 120 °C. The T_{ODT} of this mixture is determined to be ca. 105 °C.

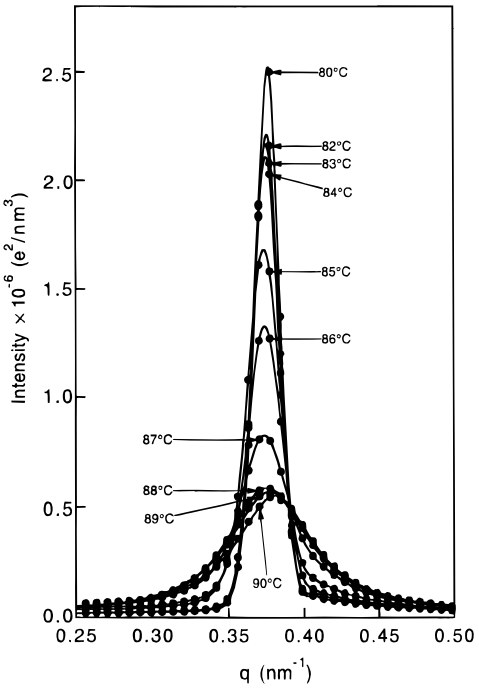

Figure 7. SAXS profiles for the 20/80 SI-M/SI-S mixture near its T_{ODT} at temperatures indicated on the plot.

It is worth noting in Figure 8 that the value of I_m in an ordered state first increases with lowering temperature from the disordered state but starts to decrease with further lowering of the temperature. This trend is seen more or less for all the samples studied here. The first trend is in line with our expectation in that ordering progresses with lowering temperature, but the

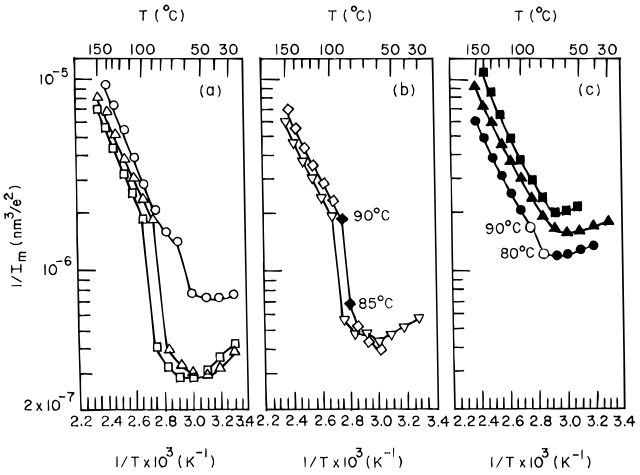

Figure 8. Plots of log ($1/I_m$) vs $1/T$ for neat block copolymers SI-S and SI-M, and their mixtures: (a) (○) neat block copolymer SI-S; (△) 20/80 SI-M/SI-S; (□) 50/50 SI-M/SI-S; (b) (▽) 65/35 SI-M/SI-S; (◇, ◆) 70/30 SI-M/SI-S; (c) (●, ○) 75/25 SI-M/SI-S; (▲) 80/20 SI-M/SI-S; (■) neat block copolymer SI-M. Low temperature-resolution SAXS experiments were performed.

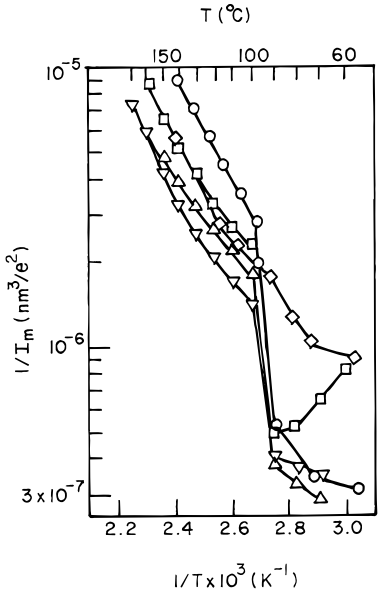

Figure 9. Plots of log ($1/I_m$) vs $1/T$ for neat block copolymers SI-Q and SI-R, and their mixtures: (○) neat block copolymer SI-R; (△) 40/60 SI-Q/SI-R; (□) 80/20 SI-Q/SI-R; (▽) 90/10 SI-Q/SI-R; (◇) neat block copolymer SI-Q. Low temperature-resolution SAXS experiments were performed.

second trend is totally unexpected because the degree of ordering is expected to level off as the temperature is decreased towards the glass transition temperature (T_g); i.e., we expected that the decreasing trend of $1/I_m$ with increasing $1/T$ (i.e., an increasing trend of I_m with decreasing temperature) would level off as the temperature approaches T_g. This intriguing trend may be interpreted, in accordance with the mechanisms suggested for polymer blends,[46,47] as being the consequence of the suppression of concentration fluctuations (and hence the scattered intensity) as the temperature of an ordered block copolymer approaches its T_g.

Figure 9 gives plots of log ($1/I_m$) vs $1/T$ for SI-Q/SI-R mixtures, obtained again with a low-temperature-resolution SAXS experiment. The data show the same trend as that given in Figure 8 for SI-M/SI-S mixtures. It should be noted that squares of the half-width at half-maximum for the first-order SAXS peaks (σ_q^2) had

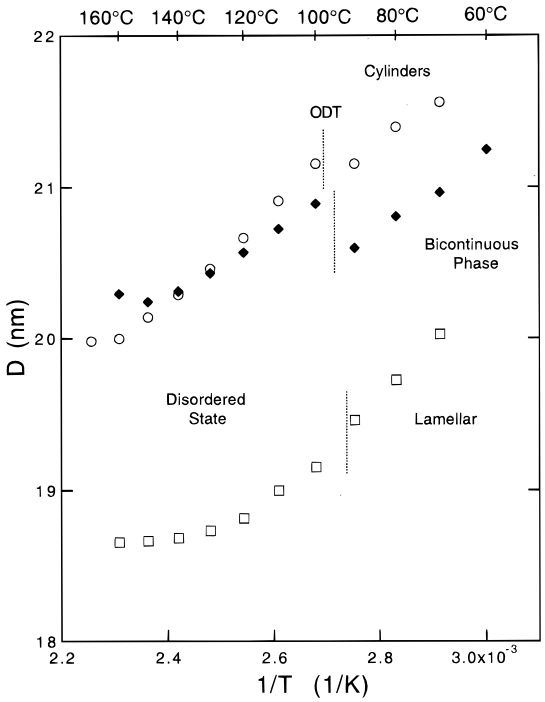

Figure 10. Plots of D vs $1/T$ for SI-Q/SI-R mixtures. (○) 90/10 SI-Q/SI-R mixture having cylindrical microdomains; (◆) 80/20 SI-Q/SI-R mixture having bicontinuous microdomains; (□) 40/60 SI-Q/SI-R mixture having lamellar microdomains.

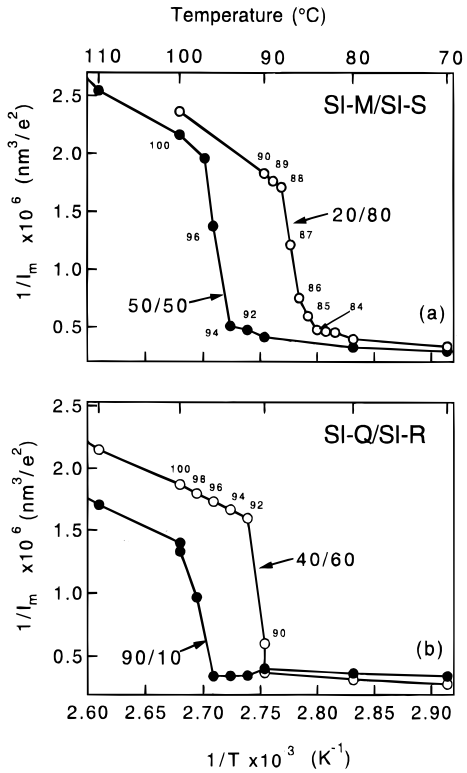

Figure 11. Plots of $1/I_m$ vs $1/T$ for (a) the 20/80 and 50/50 SI-M/SI-S mixtures and (b) 40/60 and 90/10 SI-Q/SI-R mixtures. High-temperature-resolution SAXS experiments were performed.

almost the same temperature dependence as $1/I_m$. Hence plots of σ_q^2 vs $1/T$ for SI-M/SI-S and SI-Q/SI-R mixtures are not shown here. The following observations are worth noting in Figure 9. The ODTs of 40/60, 80/20, and 90/10 SI-Q/SI-R mixtures are as sharp as the ODT of the neat block copolymer SI-R. The ODT of neat block copolymer SI-Q is not as sharp as that of neat block copolymers SI-R and their mixtures. This may be attributable to the fact that, in the ordered state, SI-Q forms hexagonally-packed cylinders of PS phase[48] which are not as regular as the lamellae formed in SI-R.[42,48] Another possibility may be that the T_{ODT} for SI-Q is too close to its T_g, so that the ordering process is slow compared to the time scale of our observation. In reference to Figure 9, at present we have no explanation as to why values of $1/I_m$ for 80/20 SI-Q/SI-R mixture increase sharply with increasing $1/T$ (i.e., with decreasing temperature) at 2.8×10^{-3} K^{-1} < $1/T$ < 3.0×10^{-3} K^{-1} in an ordered state. Note in Figure 8 that the values of $1/I_m$ for SI-M/SI-S mixtures increase with increasing $1/T$ at 3.0×10^{-3} K^{-1} < $1/T$ < 3.4×10^{-3} K^{-1}, the temperature range of which was not covered for SI-Q/SI-R mixtures. It is worth noting again that an increase of the values of $1/I_m$ with $1/T$ (observed in 80/20 SI-Q/SI-R mixture) seems to be not related to the peak shift, as pointed out earlier.

At this juncture, we briefly remark a shift of the peak position q_m, a value of q at which the SAXS intensity becomes a maximum, with temperature. For the 80/20 SI-Q/SI-R mixture, we observed that the value of q_m decreased with lowering temperature from 160 to 100 °C in the disordered state; i.e., the wavelength of the dominant mode of the concentration fluctuations (commonly referred to as Bragg spacing, D) increased with lowering temperature. Figure 10 gives plots of D vs $1/T$ for SI-Q/SI-R mixtures. Note that D is related to q_m by $D = 2\pi/q_m$. We observe from Figure 10 that for 80/20 SI-Q/SI-R mixture, D decreases discontinuously at T_{ODT} and then increases with further increasing of $1/T$ (i.e., lowering of the temperature) in the ordered state. In a previous paper,[48] we have reported a similar observation in SI block copolymers forming cylindrical microdomains. As can be seen in Figure 10, the unusual behavior of D at T_{ODT} was also observed in the 90/10 SI-Q/SI-R mixture, and this is in contrast to the continuous increase of D at T_{ODT} observed in the 40/60 SI-Q/SI-R mixture forming lamellar microdomain.

In Figure 11 are given plots of $1/I_m$ vs $1/T$ for some SI-M/SI-S mixtures (part a) and SI-Q/SI-R mixtures (part b) obtained with high-temperature-resolution SAXS experiments. We observe that the ODTs for all the mixtures shown in Figure 11 are as sharp as, or even sharper than, the ODTs of the neat block copolymer. Let us define $T_{ODT,s}$ to be the temperature at which disordering starts and $T_{ODT,c}$ to be the temperature at which disordering is completed upon increasing temperature across T_{ODT}. Then we have: (i) $T_{ODT,s} \cong$ 84 °C and $T_{ODT,c} \cong$ 88 °C for the 20/80 SI-M/SI-S mixture; (ii) $T_{ODT,s} \cong$ 94 °C and $T_{ODT,c} \cong$ 98 °C for the 50/50 SI-M/SI-S mixture; (iii) $T_{ODT,s} \cong$ 90 °C and $T_{ODT,c} \cong$ 92 °C for the 40/60 SI-Q/SI-R mixture; and (iv) $T_{ODT,s} \cong$ 96 °C and $T_{ODT,c} \cong$ 100 °C for the 90/10 SI-Q/SI-R mixture.

At temperatures between $T_{ODT,s}$ and $T_{ODT,c}$, the ordered and disordered phases coexist in a mixture, or an ordered single phase with a segregation weaker than that at $T_{ODT,s}$ fills the whole sample space in the mixture. The distinction between the two coexisting phases and the weakly segregated one phase is beyond the scope of the present study and will be left for future investigation. The distinction may be made possible by TEM on a block copolymer sample quenched very rapidly below its T_g or by ultra-small-angle X-ray scattering[49] having ultra-high spatial resolution compared to the conventional SAXS. If we define T_{ODT} to

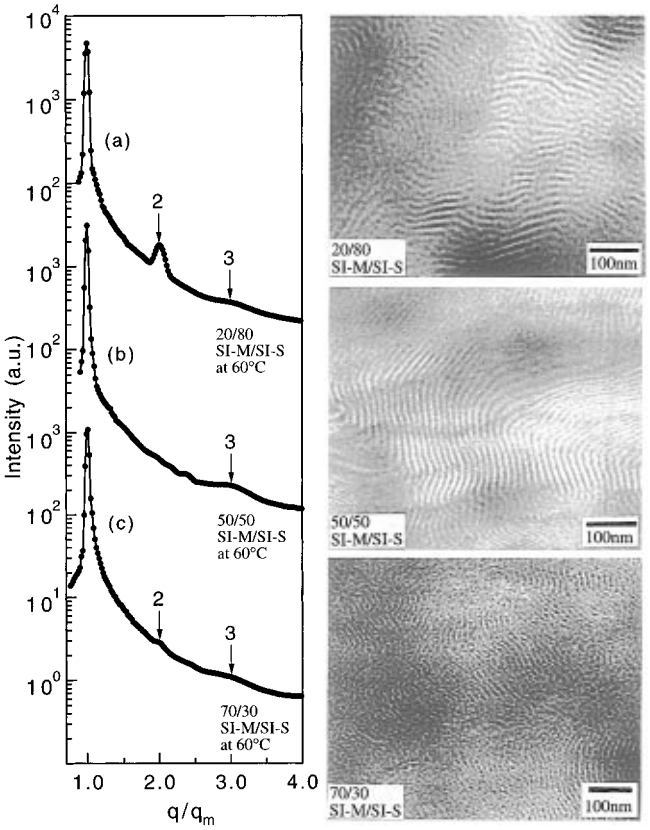

Figure 12. TEM micrographs and SAXS profiles for 20/80 SI-M/SI-S, 50/50 SI-M/SI-S, and 70/30 SI-M/SI-S mixtures.

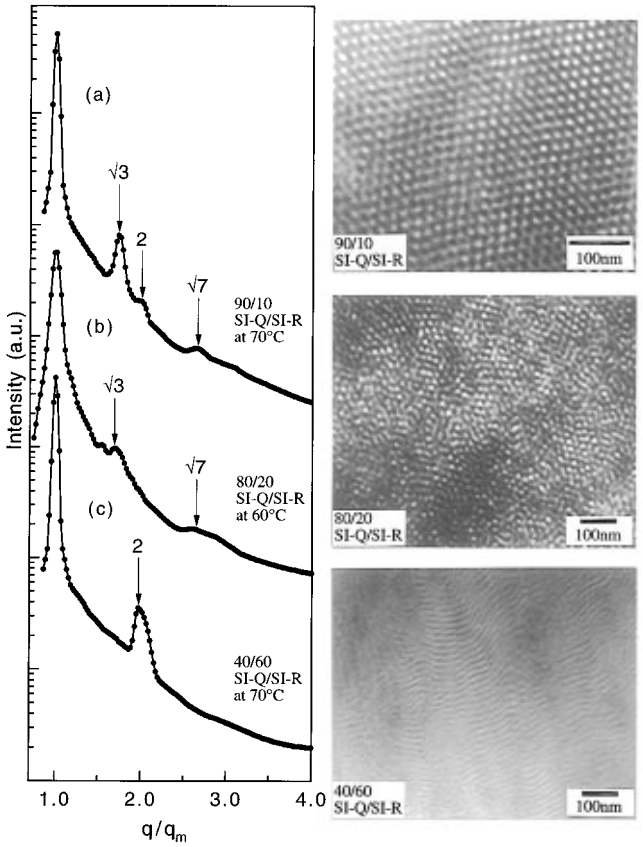

Figure 13. TEM micrographs and SAXS profiles for 90/10 SI-Q/SI-R, 80/20 SI-Q/SI-R, and 40/60 SI-Q/SI-R mixtures.

be the temperature at which the disordering is just completed, we observe (i) $T_{ODT} = 87-88$ °C for the 20/80 SI-M/SI-S mixture, (ii) $T_{ODT} = 96-98$ °C for the 50/50 SI-M/SI-S mixture, (iii) $T_{ODT} = 90-92$ °C for the 40/60 SI-Q/SI-R mixture, and (iv) $T_{ODT} = 98-100$ °C for the 90/10 SI-Q/SI-R mixture.

The sharp ODT, exhibiting discontinuous changes in I_m, σ_q^2, and q_m or D in some cases, clearly reveals an important effect of random thermal forces on ODT even for mixtures of block copolymers, as in the case of neat block copolymers. It may be possible that the thermally induced first-order phase transition in mixtures of block copolymers could develop, giving rise to a coexistence of an ordered phase and disordered phase at thermal equilibrium at or near ODT.

3.3. Microdomain Structure Investigated by TEM and SAXS. TEM observations were made on samples prepared as follows. As-cast films of each SI-M/SI-S mixture were prepared by slow evaporation of solvent from the solution consisting of 95 wt % toluene and 5 wt % polymer. The cast-films were first annealed at 80 °C (higher than the T_gs but lower than the T_{ODT}s of the mixtures) for 30 h under vacuum and then cooled slowly to room temperature and finally cut at −85 °C to ultrathin sections of ca. 50 nm thick. Basically the same procedures were used to prepare samples for taking TEM micrographs of SI-Q/SI-R mixtures.

Figure 12 gives TEM micrographs of 20/80, 50/50, and 70/30 SI-M/SI-S mixtures. Also shown in Figure 12 are SAXS profiles for the corresponding mixtures. The micrographs show that each mixture has lamellar microdomains, but some type of bicontinuous region coexists with lamellar grains. The volume fraction of lamellar grains is highest (ca. 80−90%) in the 50/50 SI-M/SI-S mixture and lowest in the 70/30 SI-M/SI-S mixture. Notice that the SAXS profiles in Figure 12 have multiple order peaks at $q/q_m = 1$, 2, and 3, indicative of lamellae, supporting the TEM results.

Note, however, that the 20/80 SI-M/SI-S mixture has a clear second-order peak, while the 50/50 SI-M/SI-S mixture does not have second-order peak. This may be explained by a minimum in the form factor of lamellae at $q/q_m = 2$ for the 50/50 SI-M/SI-S mixture; i.e., the volume fraction of each lamellar phase is close to 0.5. The 20/80 SI-M/SI-S mixture has the volume fraction of each lamella biased from 0.5, and thus, the minimum in the form factor exists at $q/q_m \neq 2$, giving rise to a second-order peak in the scattering intensity. The 70/30 SI-M/SI-S mixture has a small second-order peak, indicating that this mixture has the volume fraction of each lamella only slightly biased from 0.5.

Figure 13 gives TEM micrographs of 90/10, 80/20, and 40/60 SI-Q/SI-R mixtures. Also shown in Figure 13 are SAXS profiles for the corresponding mixtures. The TEM micrographs show that the 90/10 SI-Q/SI-R mixture has hexagonally-packed cylindrical microdomains of PS, 40/60 SI-Q/SI-R mixture has lamellar microdomains, and 80/20 SI-Q/SI-R mixture has some type of bicontinuous microdomains yet to be identified. Note in Figure 13 that the SAXS profile for the 80/20 SI-Q/SI-R mixture exhibits a broader first-order peak compared to 90/10 and 40/60 SI-Q/SI-R mixtures and it has higher order peaks at q/q_m of about $\sqrt{3}$ and $\sqrt{7}$. It is reassuring to observe in Figures 12 and 13 that TEM results are supported by independent SAXS measurements.

3.4. Phase Diagrams. Figure 14 gives phase diagrams for (a) SI-M/SI-S mixtures (including neat block copolymer SI-S) and (b) SI-Q/SI-R mixtures (including neat block copolymers SI-Q and SI-R), in terms of T_{ODT} which were determined by both rheology (●) and SAXS

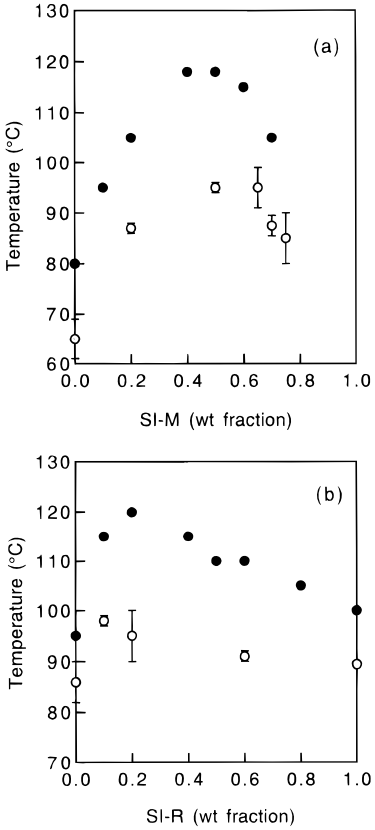

Figure 14. Phase diagrams describing order−disorder boundaries (T_{ODT}) for (a) SI-S/SI-M mixtures and (b) SI-Q/SI-R mixtures: (●) T_{ODT} determined by rheology; (○) T_{ODT} determined by SAXS. An error bar is attached to T_{ODT} determined by SAXS in the case when the error is larger than the symbol (○).

(○ with an error bar). It is of interest to observe in Figure 14 that the T_{ODT}s of all mixtures are higher than those of the constituent block copolymers and the T_{ODT}s of SI-M/SI-S mixtures are very sensitive to their composition, whereas the T_{ODT}s of SI-Q/SI-R mixtures vary relatively little with their composition (each composition has a T_{ODT}, as determined by SAXS, between 90 and 100 °C). The former trend on the T_{ODT}s of the SI-M/SI-S mixtures is due to the fact that the net composition of PS or PI block in the mixtures approaches 0.5 when the composition of SI-M in the mixtures approaches 0.5. The latter trend on the T_{ODT}s of the SI-Q/SI-R mixtures is due to a balance of the following two opposing effects of increasing the SI-R fraction on the T_{ODT}s: The increase of the SI-R fraction causes a decrease of the net molecular weight and hence a decrease of the T_{ODT}s of the mixtures, but it also causes an increase of the net composition of the PS block toward 0.5 and hence an increase of the T_{ODT}s. Notice that values of T_{ODT} determined by rheology are about 15 °C higher than those determined by SAXS. At present we cannot identify a source (sources) which may explain the discrepancy between the ODT determined by SAXS and rheology, although the oscillatory shear flow applied in the dynamic viscoelastic measurements and/or differences in the thermal protocols employed for the two different experimental methods might have something to do with it. The residual solvent can hardly account for the observed discrepancy.

Figure 15 describes the composition dependence of wavelength (D) of the dominant mode of the concentration fluctuations in the disordered state, obtained from SAXS experiments, for SI-M/SI-S mixtures and SI-Q/SI-R mixtures, where $D = 2\pi/q_m$ with q_m being the wavevector at which the scattering intensity of the sample has a maximum. In the SAXS experiment, D was measured at 150 or 160 °C, the highest temperature employed in this study. Also given in Figure 15 are, for comparison, theoretical predictions based on random phase approximation (RPA)[50] with the details of the procedures employed for obtaining the theoretical predictions given in the Appendix. It can be seen in Figure 15 that values of D from SAXS experiments are larger than those predicted from RPA. This difference may be attributable to the effect of random thermal force[51,52] or the Brazovskii effect (non-mean-field effect).[53] The effect of random thermal force on blends of block copolymers is relatively unexplored, both theoretically and experimentally, compared to that on neat block copolymers.

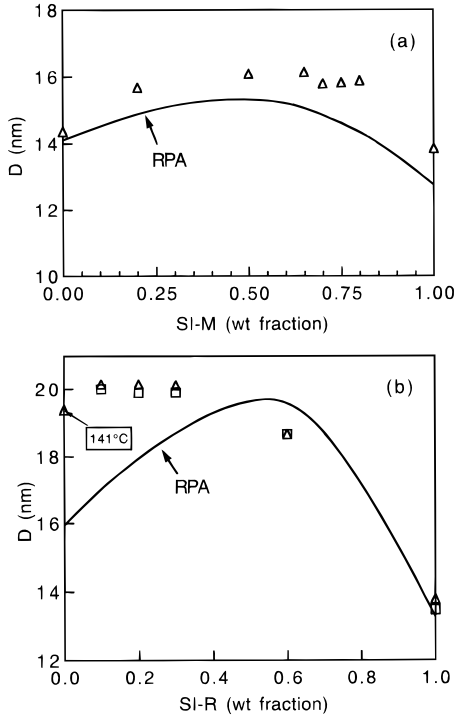

Figure 15. (a) Plots of D in the disordered state vs weight fraction of SI-M in SI-M/SI-S mixtures: (△) SAXS data at 150 °C; (—) prediction from the RPA calculation. (b) Plots of D vs weight fraction of SI-R in SI-Q/SI-R mixtures: (△) SAXS data at 150 °C except for data for neat block copolymer SI-Q taken at 141 °C; (□) SAXS data at 160 °C; (—) prediction from the RPA calculation.

Specifically, in reference to Figure 15a for SI-M/SI-S mixtures, the experimentally determined values of D are slightly larger than the theoretically predicted ones for all compositions although the general trend of the composition dependence of D is in reasonably good agreement between experiment and theory. The observed discrepancy between experiment and theory may be due to the fact that at 150 °C these mixtures have not yet reached the mean-field regime completely.[52] On the other hand, in reference to Figure 15b for SI-Q/SI-R mixtures, experimental results are in good agreement with prediction for SI-R rich (>50 wt %) mixtures but not for SI-Q rich (>89 wt %) mixtures. This may be due to the fact that the crossover temperature (T_{MF}) between the non-mean-field disordered region and the mean-field disordered region depends on blend composition, giving rise to a lower T_{MF} for SI-R rich mixtures than for SI-Q rich mixtures.

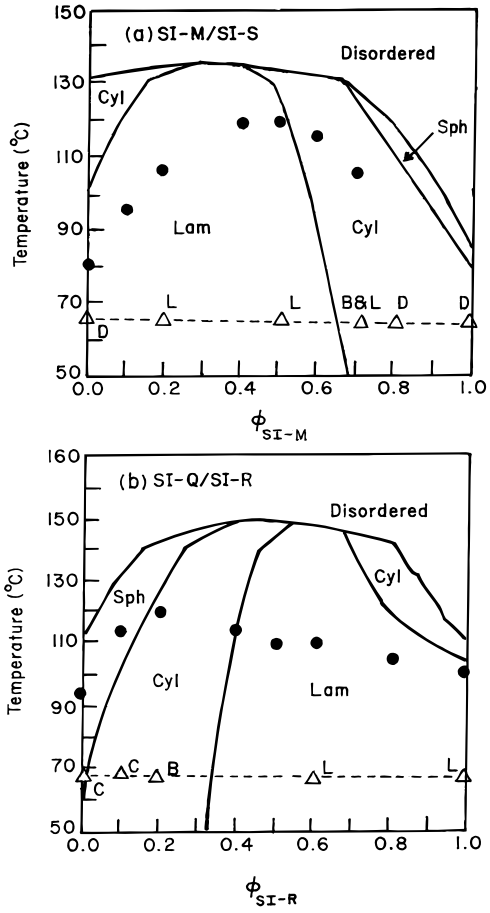

Figure 16. Comparison of phase diagrams calculated using self-consistent mean-field theory with experimental results for (a) SI-M/SI-S mixtures and (b) SI-Q/SI-R mixtures, where the solid line describes theoretically calculated order−disorder or order-order boundaries, a solid circle ● describes T_{ODT}s that were determined by rheology, and an open triangle △ describes microdomain structures that were determined by TEM in which B denotes a bicontinuous phase (although not clearly identified), C denotes a cylindrical microdomain structure, L denotes a lamellar microdomain structure, and D denotes disordered phase.

In the present study, using a self-consistent mean-field theory we constructed phase diagrams, as given by solid lines in Figure 16, which include microdomain structures in ordered states for SI-M/SI-S mixtures and SI-Q/SI-R mixtures. The details of the mean-field theory and computational procedures employed are described in a paper by Shi and Noolandi.[37] In obtaining the phase diagrams in Figure 16, we employed the following expression for the Flory−Huggins interaction parameter $\chi(T)$[54]

$$\chi(T) = -0.0937 + 66/T \qquad (1)$$

for a PS/PI pair, where T is the absolute temperature, and the following expressions

$$v_{PS} = 0.9199 + 5.098 \times 10^{-4}(T - 273) + 2.354 \times 10^{-7}(T - 273)^2 + (32.46 + 0.1017(T - 273))/M_{w,PS} \qquad (2)$$

for the specific volumes of PS,[55] where $M_{w,PS}$ is the molecular weight of PS, and

$$v_{PI} = 1.0771 + 7.22 \times 10^{-4}(T - 273) + 2.46 \times 10^{-7}(T - 273)^2 \qquad (3)$$

for the specific volume of PI.[44] In eqs 2 and 3, v_{PS} and v_{PI} have units of centimeter cubed per gram. Also given in Figure 16 are, for comparison, experimental values of T_{ODT} which were obtained by rheology measurements (●). In Figure 16 we observe that the order−disorder boundaries predicted by theory are higher (15−40 °C) than those obtained by experiment. However, the general trend of the composition dependence of the order−disorder boundaries is in reasonably good agreement between theory and experiment. We hasten to point out that different values of the constants appearing in eq 1 (see, for example, ref 42) may give rise to differently shaped order−disorder boundaries.

For comparison, experimentally determined microdomain structures (△) are indicated in Figure 16. From Figure 16a we observe that the self-consistent mean-field theory correctly predicts the existence of the lamellar microdomain structure in 50/50 and 20/80 SI-M/SI-S mixtures. The theory predicts the hexagonally-packed cylindrical microdomain morphology in the 70/30 SI-M/SI-S mixture, whereas the TEM picture (see Figure 12) shows some type of bicontinuous microdomain structure containing 20−30% of lamellar grains dispersed in the matrix of the bicontinuous structure. Notice in Figure 16a that the experimentally observed microdomain structure lies very close to the phase boundary between cylindrical microdomains and lamellar microdomains. The theory predicts a lamellar microdomain structure for the neat block copolymer SI-S and cylindrical morphology for the neat block copolymer SI-M. However, the experimental results show that neat block copolymers SI-S and SI-M are in the disordered state at 65 °C. From Figure 16b we observe that the self-consistent mean-field theory correctly predicts the experimentally observed microdomain structure, namely, hexagonally-packed cylindrical microdomains in the neat block copolymer SI-Q and 90/10 SI-Q/SI-R mixture and lamellae in the 40/60 SI-Q/SI-R mixture and neat block copolymer SI-R.[42] The theory predicts the existence of the hexagonally-packed cylindrical microdomain morphology in the 80/20 SI-Q/SI-R mixture, whereas the TEM picture (see Figure 13) shows some type of bicontinuous microdomain structure which is yet to be identified.

It is worth noting at this juncture that Zhao et al.[56] investigated the phase behavior of binary mixtures of poly(ethylene)-*block*-poly(ethylethylene) (PE-*block*-PEE) copolymers and speculated on the existence of biphasic or triphasic regions at the order−order phase boundaries. They remarked that mean-field theory predicted a very narrow two-phase region in their polymer systems. The coexistence of lamellar and bicontinuous microdomains in the 70/30 SI-M/SI-S mixture, shown in Figure 12, seems to correspond to the biphasic region speculated by Zhao et al.[56]

It should be emphasized that the theoretical phase diagrams presented in Figure 16, which are based on a self-consistent mean-field theory, were constructed without having any adjustable parameters. In this regard, the self-consistent mean-field theory may be regarded as being reasonably successful in capturing the major features of phase behavior in binary mixtures of SI diblock copolymers. Needless to say, the phase behavior

of such mixtures is indeed much more complex than that of homopolymer mixtures.

4. Concluding Remarks

In this paper we have presented ODT, microdomain structure, and phase diagrams for binary mixtures of SI diblock copolymers having different microdomain structures. We determined the T_{ODT}s of neat block copolymers and their binary mixtures by rheology (i.e., log G' vs log G'' plots) and SAXS, respectively. The microdomain structure of some binary mixtures determined by SAXS agrees well with that determined by TEM. We observed, however, that certain binary mixtures of SI diblock copolymers give rise to a very complex microdomain structure, which is yet to be identified.

The SAXS results reveal a sharp ODT, showing discontinuous changes in scattering properties (I_m and σ_q^2), for binary mixtures of block copolymers as in the case of neat block copolymers. This indicates that ODT is significantly affected by random thermal forces (thermally induced first-order phase transition). The ODT was found to occur over a finite range of temperatures ($\Delta T = T_{ODT,c} - T_{ODT,s} \leq 4$ °C), suggesting either the coexistence between the ordered and disordered phases or the existence of an ordered single phase with varying amplitudes of concentration fluctuations over ΔT. Although it is left for future investigation to determine which of the two possibilities is more likely to occur, at present we speculate from the point of view of random thermal force effects that the former possibility is more likely to occur than the latter possibility. We are of the opinion, on the basis of our previous experimental studies, that the rheology is not effective in differentiating between coexisting phases and a weakly segregated one-phase region. Of course, the rheology is very effective in differentiating between the microphase-separated phase and the homogeneous phase, as can be seen in Figures 1−3.

In this study, using a self-consistent mean-field theory, we calculated equilibrium phase diagrams and microdomain structures in binary mixtures of SI diblock copolymers, namely SI-M/SI-S and SI-Q/SI-R mixtures. When compared with experimental results, the self-consistent mean-field theory predicts, with some exceptions, a reasonably accurate microdomain structure in binary mixtures of SI diblock copolymers. We found that the order−disorder boundaries calculated from the self-consistent mean-field theory are higher (by 15−40 °C) than those determined by rheological measurements. The observed difference between theory and experiment may be attributable, among many factors, to the various assumptions made in the self-consistent mean-field theory and the specific numerical values of the coefficients, A and B, appearing in the expression for the Flory−Huggins interaction parameter: $\chi(T) = A + B/T$. Several research groups reported on different values of A and B for PS/PI pair, which should lead to different order−disorder boundaries for a given binary mixture of SI diblock copolymers. On the other hand, it is also possible to use A and B as fitting parameters in the self-consistent mean-field theory, which would lead to better agreement between theory and experiment.

Appendix. RPA Employed for Calculations of the Wavelength D of the Dominant Mode of Fluctuations in Binary Mixtures of AB-Type Diblock Copolymers

Below we describe the procedures employed in this study for calculating values of D from the scattering function, $I(q)$, of the disordered melt consisting of two AB-type diblock copolymers, i.e., $(A-B)_\alpha/(A-B)_\beta$ diblock copolymer mixtures, with polydispersities in molecular weight and asymmetries in segmental volume. The $I(q)$ has a maximum at a particular value of wavevector **q**, q_m.

According to Leibler,[50] a general formula for $I(q)$ for an AB-type diblock copolymer in the disordered state is given by

$$1/I(q) \propto S(q)/W(q) - 2\chi \tag{A1}$$

where

$$S(q) = S_{AA}(q) + S_{BB}(q) + 2S_{AB}(q) \tag{A2}$$

$$W(q) = S_{AA}(q)S_{BB}(q) - S_{AB}(q)^2 \tag{A3}$$

in which χ is the interaction parameter and q is the magnitude of **q** defined by

$$q = (4\pi/\lambda)\sin(\theta/2) \tag{A4}$$

where λ is the wavelength of the incident X-ray and θ is the scattering angle.

For $(A-B)_\alpha/(A-B)_\beta$ mixtures, we have

$$S_{AA}(q) = \Phi_\alpha r_\alpha (f_{A\alpha})^2 g_{A\alpha}{}^{(2)} + \Phi_\beta r_\beta (f_{A\beta})^2 g_{A\beta}{}^{(2)} \tag{A5}$$

$$S_{BB}(q) = \Phi_\alpha r_\alpha (f_{B\alpha})^2 g_{B\alpha}{}^{(2)} + \Phi_\beta r_\beta (f_{B\beta})^2 g_{B\beta}{}^{(2)} \tag{A6}$$

$$S_{AB}(q) = \Phi_\alpha r_\alpha f_{A\alpha} g_{A\alpha}{}^{(1)} f_{B\alpha} g_{B\alpha}{}^{(1)} + \Phi_\beta r_\beta f_{A\beta} g_{A\beta}{}^{(1)} f_{B\beta} g_{B\beta}{}^{(1)} \tag{A7}$$

where Φ_i (i = α or β) is the volume fraction of the i-th polymer in the $(A-B)_\alpha/(A-B)_\beta$ mixture with $\Phi_\alpha + \Phi_\beta = 1$; $r_i = (v_A/v_o)N_{Ai} + (v_B/v_o)N_{Bi}$ (i = α or β) is the effective degree of polymerization of the i-th polymer (we take the asymmetries in segmental volume into consideration) in which $v_o = (v_A v_B)^{1/2}$ and v_j (j = A or B) is the molecular volume of the j-th monomer and N_{ji} is the weight-average degree of polymerization of the j-th block in the i-th polymer; f_{ji} (j = A or B, i = α or β) is the volume fraction of the j-th block in the i-th polymer with $f_{Ai} = N_{Ai}v_A/(N_{Ai}v_A + N_{Bi}v_B)$ and $f_{Bi} = N_{Bi}v_B/(N_{Ai}v_A + N_{Bi}v_B)$; $g_{ji}^{(1)} = \{1 - [x_{ji}(\lambda_i - 1) + 1]^{-1/(\lambda_i - 1)}\}/x_{ji}$ (j = A or B, i = α or β); $g_{ji}^{(2)} = 2\{-1 + x_{ji} + [x_{ji}(\lambda_i - 1) + 1]^{-1/(\lambda_i - 1)}\}/x_{ji}^2$ (j = A or B, i = α or β); $x_{ji} = (N_{ji}b_j^2/6)q^2$ with b_j being the segment length of j-th block chain; $\lambda_i = \{[(M_w/M_n)_i - 1]/(w_{Ai}^2 + w_{Bi}^2)\} + 1$ (i = α or β) with $(M_w/M_n)_i$ being the polydispersity index in molecular weight of the i-th polymer and w_{ji} being the weight fraction of the j-th block in the i-th polymer defined by M_{wji}/M_{wi} with M_{wji} being the weight-average molecular weight of the j-th block in the i-th polymer and M_{wi} being the weight-average molecular weight of the i-th polymer.

In the calculations, suffixes A and B should be replaced by the suffixes PS (denoting polystyrene) and PI (denoting polyisoprene), respectively. The values of v_{PS} and v_{PI} were calculated at a fixed temperature of 423 K by using eqs 2 and 3, respectively. This temperature is well above the T_{ODT}s of the mixtures employed

in our experiment. Following the previous study,[42] we used $b_{PS} = 0.68$ nm and $b_{PI} = 0.63$ nm. Using these values for v_{PS}, v_{PI}, b_{PS}, and b_{PI}, together with the values of other parameters listed in Table 1, we can calculate the scattering function $I(q)$ for SI-M/SI-S and SI-Q/SI-R mixtures in the disordered state. The scattering functions for all the mixtures show a single scattering maximum q_m, and the wavelength D of the dominant mode of the fluctuations was estimated from $D = 2\pi/q_m$ and plotted in Figure 15.

Acknowledgment. A.-C.S. wishes to acknowledge useful discussions that he had with Dr. Jaan Noolandi.

References and Notes

(1) Zin, W.-C.; Roe. R. J. *Macromolecules* **1984**, *17*,183.
(2) Nojima, S.; Roe, R.-J. *Macromolecules* **1987**, *20*, 1866.
(3) Kim, J.; Han, C. D.; Chu, S. G. *J. Polym. Sci., Polym. Phys. Ed*. **1988**, *26*, 677.
(4) Owens, J. N.; Gancarz, I. S.; Koberstein, J. T.; Russell, T. P. *Macromolecules* **1989**, *22*, 3388.
(5) Han, C. D.; Kim, J.; Baek, D. M.; Chu, S. G. *J. Polym. Sci., Polym. Phys. Ed.* **1990**, *28*, 315.
(6) Hashimoto, T. Tanaka, H.; Hasegawa, H.; *Macromolecules* **1990**, *23*, 4378.
(7) Tanaka, H.; Hasegawa, H.; Hashimoto, T. *Macromolecules* **1991**, *24*, 240.
(8) Tanaka, H.; Hashimoto, T. *Macromolecules* **1991**, *24*, 5713.
(9) Winey, K. I.; Thomas, E. L.; Fetters, L. J. *J. Chem. Phys.* **1991**, *95*, 9367.
(10) Koizumi, S.; Hasegawa, H.; Hashimoto, T. *Macromol. Chem., Macromol. Symp.* **1992**, *62*, 75.
(11) Hashimoto, T.; Koizumi, S.; Hasegawa, H.; Izumitani, T.; Hyde, S. T. *Macromolecules* **1992**, 25, 1433.
(12) Winey, K. I.; Thomas, E. L.; Fetters, L. J. *Macromolecules* **1992**, *25*, 422.
(13) Disko, M. M.; Liang, K. S.; Behal, S. K.; Roe, R. J.; Jeon, K. J. *Macromolecules* **1993**, 26, 2983.
(14) Spontak, R. J.; Smith, S. D.; Ashraf, A. *Macromolecules* **1993**, 26, 956.
(15) Spontak, R. J.; Smith, S. D.; Ashraf, A. *Macromolecules* **1993**, 26, 5118.
(16) Koizumi, S.; Hasegawa, H.; Hashimoto, T. *Macromolecules* **1994**, *27*, 6532.
(17) Löwenhaupt, B.; Steurer, A.; Hellmann, G. P.; Gallot, Y. *Macromolecules* **1994**, *27*, 908.
(18) Hong, K. M.; Noolandi, J. *Macromolecules* **1983**, *16*, 1083.
(19) Roe, R. J.; Zin, W.-C. *Macromolecules* **1984**, *17*, 189.
(20) Whitmore, M. D.; Noolandi, J. *Macromolecules* **1985**, *18*, 2486.
(21) Han, C. D.; Baek, D. M.; Kim, J.; Kimishima, K.; Hashimoto, T. *Macromolecules* **1992**, *25*, 3052.
(22) Baek, D. M.; Han, C. D.; Kim, J. K. *Polymer* **1992**, *33*, 4821.
(23) Winey, K. I.; Thomas, E. L.; Fetters, L. J. *Macromolecules* **1992**, *25*, 2645
(24) Kang, C.-K.; Zin, W.-C. *Macromolecules* **1992**, *25*, 3039.
(25) Semenov, A. N. *Macromolecules* **1993**, *26*, 2273.
(26) Mayes, A. M.; Russell, T. P.; Satija, S. K.; Majkrzak, C. F. *Macromolecules* **1992**, *25*, 6523.
(27) Shull, K. R.; Winey, K. I. *Macromolecules* **1992**, *25*, 2637.
(28) Kimishima, K.; Hashimoto, T.; Han, C. D. *Macromolecules* **1995**, *28*, 3842.
(29) Hashimoto, T.; Tanaka, H.; Hasegawa, H.; In *Molecular Conformation and Dynamics of Macromolecules in Condensed Systems*; Nagasawa, M., Ed., Elsevier: Amsterdam, 1988; p 257.
(30) Ishizu, K.; Omote, A.; Fukutomi, T. *Polymer* **1990**, 31, 2135.
(31) Hashimoto, T.; Yamasaki, K. Koizumi, S.; Hasegawa, H. *Macromolecules* **1993**, *26*, 2895.
(32) Hashimoto, T.; Koizumi, S.; Hasegawa, H. *Macromolecules* **1994**, *27*, 1562.
(33) Koizumi, S.; Hasegawa, H.; Hashimoto, T. *Macromolecules* **1994**, *27*, 4371.
(34) Lyatskaya, Ju. V.; Zhulina, E. B.; Birshtein, T. M. *Polymer* **1992**, *33*, 343, 2750.
(35) Dan, N.; Safran, S. A. *Macromolecules* **1994**, *27*, 5766.
(36) Shi, A.-C.; Noolandi, J. *Macromolecules* **1994**, *27*, 2936.
(37) Shi, A.-C.; Noolandi, J. *Macromolecules* **1995**, *28*, 3103.
(38) Mayes, A. M.; Russell, T. P.; Deline, V. R.; Satija, S. K.; Majkrzak, C. F. *Macromolecules* **1994**, *27*, 7447.
(39) (a) Hashimoto, T.; Suehiro, S.; Shibayama, M.; Saijo, K.; Kawai, H. *Polym. J.* **1981**, *13*, 501. (b) Suehiro, S.; Saijo, K.; Ohta, Y.; Hashimoto, T.; Kawai, H. *Anal. Chim. Acta* **1986**, *189*, 41.
(40) Fujimura, M.; Hashimoto, T.; Kawai, H. *Mem. Fac. Eng., Kyoto Univ.* **1981**, *43* (2), 224.
(41) Hendricks, R. W. *J. Appl. Crystallogr.* **1972**, *5*, 315.
(42) Han, C. D.; Baek, D. M.; Kim, J. K.; Ogawa, T.; Sakamoto, N.; Hashimoto, T. *Macromolecules* **1995**, *28*, 5043.
(43) Han, C. D.; Kim, J. *J. Polym. Sci. Part B: Polym. Phys.* **1987**, *25*, 1741.
(44) Han, C. D.; Kim, J.; Kim, J. K. *Macromolecules* **1989**, *22*, 383.
(45) Han, C. D.; Baek, D. M.; Kim, J. K. *Macromolecules* **1990**, *23*, 561.
(46) Khokhlov. A. R.; Erukhimovich, I. Y. *Macromolecules* **1993**, *26*, 7195.
(47) Takeno, H.; Koizumi, S.; Hasegawa, H.; Hashimoto, T. *Macromolecules* **1996**, *29*, 2440.
(48) Ogawa, T.; Sakamoto, N.; Hashimoto, T.; Han, C. D.; Baek, D. M. *Macromolecules* **1996**, *29*, 2113.
(49) (a) Bouse, U.; Hart, M. *Z. Phys.* **1965**, *189*, 151. (b) Koga, T.; Hart, M.; Hashimoto, T. *J. Appl. Cryst.* **1996**, *29*, 318. (c) Koga, T.; Koga, T.; Hashimoto, T. in preparation.
(50) Leibler, L. *Macromolecules* **1980**, *13*, 1602.
(51) Fredrickson, G. H.; Helfand, E. *J. Chem. Phys.* **1987**, *87*, 697.
(52) Sakamoto, N.; Hashimoto, T. *Macromolecules* **1995**, *28*, 6825.
(53) Brazovskii, A. *Sov. Phys.-JETP* **1975**, *41*, 85.
(54) Mori, K.; Hasegawa, H.; Hashimoto, T. *Polym. J.* **1985**, *17*, 799.
(55) Richardson, M. J.; Savill, N. G. *Polymer* **1977**, *18*, 3.
(56) Zhao, J.; Majumdar, B.; Schulz, M. F.; Bates, F. S.; Almdal, K.; Mortensen, K.; Hajduk, D. A.; Gruner, S. M. *Macromolecules* **1996**, *29*, 1204.

MA970050X